

AD 749330

NOLTR 72-82

THE MEASUREMENT OF PARTICLE VELOCITY  
IN PRESSED TNT

By  
D. J. Edwards  
J. O. Erkman  
Donna Price

18 AUGUST 1972

NOL

D D C  
RECEIVED  
18 AUG 1972  
A

NAVAL ORDNANCE LABORATORY, WHITE OAK, SILVER SPRING, MARYLAND

BEST  
AVAILABLE COPY

APPROVED FOR PUBLIC RELEASE;  
DISTRIBUTION UNLIMITED

NATIONAL TECHNICAL  
INFORMATION SERVICE

NOLTR 72-82

Unclassified

Security Classification

## DOCUMENT CONTROL DATA - R &amp; D

(Security classification of title, body of abstract and indexing annotation must be entered when the overall report is classified)

|   |  |   |                       |
|---|--|---|-----------------------|
| 1. ORIGINATING ACTIVITY (Corporate author)<br>NAVAL ORDNANCE LABORATORY<br>White Oak, Silver Spring, Md. 20910  |  | 2a. REPORT SECURITY CLASSIFICATION<br>Unclassified                                    |                       |
|   |  | 2b. GROUP   |                       |
| 3. REPORT TITLE<br>The Measurement of Particle Velocity in Pressed TNT  |  |   |                       |
| 4. DESCRIPTIVE NOTES (Type of report and inclusive dates)   |  |   |                       |
| 5. AUTHOR(S) (First name, middle initial, last name)<br>D. J. Edwards, J. O. Erkman and Donna Price   |  |   |                       |
| 6. REPORT DATE<br>18 August 1972  |  | 7a. TOTAL NO. OF PAGES<br>39  | 7b. NO. OF REFS<br>12 |
| 8a. CONTRACT OR GRANT NO.   |  | 8a. ORIGINATOR'S REPORT NUMBER(S)<br>NOLTR 72-82                                      |                       |
| b. PROJECT NO.<br>MAT-03L-000/ZR011-01-01   |  |   |                       |
| c.  |  | 9b. OTHER REPORT NO(S) (Any other numbers that may be assigned this report)           |                       |
| d.  |  |   |                       |
| 10. DISTRIBUTION STATEMENT<br>Approved for public Release; distribution unlimited.  |  |   |                       |
| 11. SUPPLEMENTARY NOTES   |  | 12. SPONSORING MILITARY ACTIVITY<br>Naval Material Command<br>Washington, D. C. 20360 |                       |
| 13. ABSTRACT<br>The electromagnetic velocity (EMV) gage was used to record the particle velocity as a function of time behind detonation fronts in pressed TNT. Reproducible estimates of the reaction time and of the Chapman-Jouguet particle velocity are obtainable from single records. This is in contrast to the work with cast TNT, where the breaks in the u,t curves were much more obscure. For pressed TNT at $1.60 \pm 0.01$ gm/cc in 50.8 mm diameter cylinders, the measured value of $u_{CJ}$ is $1.72$ mm/ $\mu$ sec; the reaction time is 141 nanoseconds. The value of $u_{CJ}$ reported above is 7.5% higher than the value found for cast TNT at a density of 1.62 gm/cc. The reaction time is less than half that of cast TNT. For a similar pressed TNT, Dremin reported a value of $u_{CJ}$ of $1.62$ mm/ $\mu$ sec and a reaction time of < 100 nanoseconds. The difference between the Russian results and ours is attributed to the faster rise time of our oscilloscopes. |  |   |                       |

DD FORM 1473

(PAGE 1)

S/N 0101-807-6801

UNCLASSIFIED

Security Classification

**Security Classification**

DD FORM 1473 (BACK)  
(PAGE 2)

**UNCLASSIFIED**  
Security Classification

ib

THE MEASUREMENT OF PARTICLE VELOCITY  
IN PRESSED TNT

By:

D. J. Edwards, J. O. Erkman and Donna Price

**ABSTRACT:** The electromagnetic velocity (EMV) gage was used to record the particle velocity as a function of time behind detonation fronts in pressed TNT. Reproducible estimates of the reaction time and of the Chapman-Jouguet particle velocity are obtainable from single records. This is in contrast to the work with cast TNT, where the breaks in the  $u, t$  curves were much more obscure. For pressed TNT at  $1.60 \pm 0.01$  gm/cc in 50.8 mm diameter cylinders, the measured value of  $u_{CJ}$  is 1.72 mm/ $\mu$ sec; the reaction time is 141 nanoseconds. The value of  $u_{CJ}$  reported above is 7.5% higher than the value found for cast TNT at a density of 1.62 gm/cc. The reaction time is less than half that of cast TNT. For a similar pressed TNT, Dremin reported a value of  $u_{CJ}$  of 1.62 mm/ $\mu$ sec and a reaction time of <100 nanoseconds. The difference between the Russian results and ours is attributed to the faster rise time of our oscilloscopes.

NOLTR 72-82

18 August 1972

**THE MEASUREMENT OF PARTICLE VELOCITY IN PRESSED TNT**

The work described in this report was carried out under IR159, Task MAT-031-000/ZR011-01-01 (Transition from Deflagration to Detonation) of the Naval Ordnance Laboratory's (NOL's) Independent Research Program.

The work described is the measurement of particle velocity in detonating pressed TNT by the electromagnetic velocity gage technique. The value of the Chapman-Jouguet particle velocity is about 6% greater than the value reported in the Russian literature.

ROBERT WILLIAMSON II  
Captain, USN  
Commander

*100 1.1.1 72-82*  
ALBERT LIGHTBODY  
By direction

# CONTENTS

|   | Page |
|---|------|
| INTRODUCTION.....   | 1    |
| EXPERIMENTAL.....   | 1    |
| Material.....   | 1    |
| Experimental Setup.....                                       | 2    |
| Instrumentation and Data Reduction.....                       | 2    |
| Effect of Size of the PWB on Triggering of Oscilloscopes..... | 2    |
| RESULTS AND DISCUSSION.....                                   | 2    |
| Factors Which Affect Records and Their Interpretation.....    | 2    |
| Evaluation of Single Record Results.....                      | 2    |
| Pair Comparison of u,t Curves.....                            | 5    |
| Consideration of Different Record Treatments.....             | 5    |
| Buildup of Particle Velocity with Charge Length.....          | 6    |
| Appearance of Additional Break at ~600 ns.....                | 6    |
| COMPARISON OF PRESSED AND CAST TNT RESULTS.....               | 6    |
| COMPARISON WITH PREVIOUS TNT RESULTS.....                     | 7    |
| SUMMARY AND CONCLUSIONS.....                                  | 8    |
| APPENDIX.....   | A11  |

# ILLUSTRATIONS

| Figure | Title  | Page |
|--------|--|------|
| 1      | Experimental Setup.....                          | 1    |
| 2      | Comparison of Different Thickness EMV Gages..... | 2    |
| 3      | u,t Curve with One Break.....                    | 12   |

# NOLTR 72-82

## CONTENTS (Continued)

| Figure | Title   | Page |
|--------|---|------|
| 4      | u,t Curve with Two Breaks.....  | 13   |
| 5      | TNT/PMMA Interface Result (x = 25.4 mm).....  | 14   |
| 6      | Impedance Matching Calculation for Pressed TNT/PMMA Interface Result (x = 25.4 mm)..... | 15   |
| 7      | C-J Particle Velocity vs Distance.....  | 16   |

## TABLES

| Table | Title   | Page |
|-------|---|------|
| 1     | List of Individual Experiments.....   | 17   |
| 2     | C-J Values From Break Point on Individual Records.....                        | 18   |
| 3     | u <sub>CJ</sub> Values Obtained by Method of Plane Taylor Wave Comparison.... | 19   |
| 4     | Pair Comparison of u,t Curves.....  | 20   |
| 5     | Overall Results for Pressed TNT.....  | 21   |
| 6     | Detonation Parameters of Cast and Pressed TNT.....                            | 22   |
| 7     | Comparison of Pressed TNT Results.....  | 23   |
| 8     | Measured Pressure for Composition B-3.....                                    | 24   |
| A1    | Records with Two Breaks.....  | 42   |
| A2    | Pair Comparison for Cast TNT.....   | 13   |

## INTRODUCTION

The particle velocity ( $u$ ) vs time ( $t$ ) behavior of detonating pressed TNT has been investigated by using the electromagnetic velocity (EMV) gage. The particle velocity is obtained by measuring the emf developed across the base of the EMV gage which is moving with the detonation products in a magnetic field (Figure 1). The magnetic field is oriented normal to the direction of the gage base and the direction of motion. The emf generated across the gage base, in volts, is

$$V = H u \ell \times 10^{-4}$$

where  $H$  is the magnetic field in gauss,  $u$  is in mm/ $\mu$ sec, and  $\ell$  is the gage base length in mm. The EMV gage and associated instrumentation are described in previous reports.<sup>1,2</sup> Results obtained with the EMV gage in a non-conductor (PMMA) agreed to within experimental error with previous work in which a high speed camera was used.

The Chapman-Jouguet (C-J) parameters of high density pressed TNT have been a subject of dispute for several years.<sup>3,4,5</sup> Specifically, the C-J particle velocity and pressure determined by Dremin<sup>3,4</sup> with the EMV gage are 15% lower than the values reported by Craig<sup>5</sup> who used a free surface velocity technique. One objective of this study was to determine which of the previous investigations was the more accurate.

A second objective of this study was to answer two questions: (1) Could an abrupt change of slope (break) be observed in the initial part of individual  $u, t$  records for high density pressed TNT? Dremin<sup>3,4</sup> was unable to see such a break in high density pressed TNT or any other high density pressed explosive, probably because of the limitations of his oscilloscopes. Our oscilloscopes have rise times as short as 2.3 ns so their response is not a limiting factor in our work; (2) If this break is observed, could it confidently be called the C-J point? If it could, the number of experiments needed to determine the C-J parameters would be significantly reduced.

A final objective was to compare the C-J parameters and particle velocity-time behavior of pressed and cast TNT<sup>6</sup> at approximately the same density.

## EXPERIMENTAL

**Material.** The TNT used in this work was granular, Grade 1 (90% passes through a Number 50 screen). The average particle size is 200 $\mu$ . The TNT, batch X517, was pressed isostatically at 30,000 psi to produce charges at



a density of  $1.60 \pm 0.01$  g/cc. The reported detonation velocity is  $6.91$  mm/ $\mu$ sec.<sup>4\*</sup> The pressed pellets were machined to a diameter of 50.8 mm and to the required length,  $x$  ( $25.4 \leq x \leq 76$  mm).

**Experimental Setup.** The explosive charge and booster configuration used in this work are shown in Figure 1. Baratol-Pentolite plane wave boosters, PWB (50.8 or 63.5 mm diameter), were used in all experiments to initiate the pressed TNT directly. The PWB was initiated by a primacord lead (120 grain/foot, RDX) 30 cm long which in turn was initiated by an exploding bridgewire detonator. The primacord isolates the charge from the detonator in order to prevent possible stray electrical signals from the firing unit from being picked up by the gage.

The EMV gage consists of a rectangular loop of aluminum foil 0.13 mm (5 mils) thick and  $\sim 5$  mm wide. It is mounted in a pressed TNT back-up assembly whose thickness,  $F$ , is 25.4 mm. The length of the base of the gage,  $L$ , is determined by the width, 10 mm, of piece B in Figure 1. The gage is mounted in the pressed TNT by shaping the foil around piece B; a thin layer of silicone grease is placed on pieces B, C, and D except near the gage; then pieces B, C, and D are placed together and cemented in place under a slight pressure; Duco cement is used. The gage circuit is completed by connecting the foil leads (30-35 mm length) to an RG 58 C/U coaxial line (50 ohms nominal impedance) with a 50 ohm resistor in series with the foil.

A 0.13 mm thick, 6.4 cm square aluminum baffle (see Figure 1) is located in the plane of the PWB-pressed TNT interface. This baffle helps to reduce electrical noise as is described in reference 6. The magnets, constant voltage power supply, and magnetic field measuring technique are also described in reference 6. About one third of the experiments were conducted using a constant current power supply. Replicate shots where the power supply was the only difference gave results which agreed to within reading error ( $\pm 1\%$ ).

**Instrumentation and Data Reduction.** The instrumentation and data reduction used in this study are exactly the same as those described in references 2 and 6.

**Effect of Size of the PWB on Triggering of Oscilloscopes.** In our work, the oscilloscopes were set up to self trigger on the signal from the gage. This method of triggering worked when the diameter of the PWB was the same as that of the charge (50.8 mm). When we used larger diameter boosters (63.5 mm), the oscilloscopes triggered before the detonation front reached the gage. This was apparently due to an electrical signal being generated by gas products from the larger diameter PWB; the expanding gases probably flow along the sides of the pressed TNT charge. The spurious signal was not suppressed when the assembly of unequal diameter charger was placed in mineral oil as suggested by the work of Hayes.

## RESULTS AND DISCUSSION

A total of 27 experiments were made using pressed TNT,  $\rho_0 = 1.60$  gm/cc; of these, results of five were discarded because of oscilloscope malfunction.

\*This value from Russian measurements is within 0.02 mm/ $\mu$ sec of all generally accepted infinite diameter D values.

The primary malfunction was a lengthening of the rise time caused by a bad resistor. The experiments used in the following discussion are listed in Table 1.

Factors Which Affect Records and Their Interpretation. When interpreting EMV gage records, there are two main factors to consider: (a) conduction (which will be discussed below) and (b) rise time. At least five factors contribute to the rise time:

1. Shock impedance mismatch
2. Inherent rise time of the oscilloscopes
3. Electrical impedance mismatch
4. Wave front tilt
5. Wave front curvature

A detailed discussion of these effects and their relation to rise time,  $T_0$ , is given in reference 2 and 6. In the present study, the magnitude of the last two effects has to be determined. In one experiment, we examined the wave front after it had traveled from a PWB booster through 25.4 mm of pressed TNT (both 50.8 mm diameter); it was plane but was tilted 0.8 mm over the middle 20 mm. The resulting calculated value of  $T_0$  is then 85 or 125 ns depending on whether two or three double reflections are used for factor 1. All of our records show a rise time of less than 125 ns with most of them closer to 85 ns.

In the study of cast TNT<sup>6</sup>, it was pointed out that a knowledge of the conduction of the detonation products of the particular explosive under study is needed to determine the thickness of the EMV gage to be used. In order to determine the optimum gage thickness for high density pressed TNT, experiments were performed with gage thicknesses of 1, 3, and 5 mils. As can be seen from Figure 2, the 1 mil curve lies considerably below the 3 and 5 mil curves. This is believed due to the higher resistance of the 1 mil gage; this resistance is further increased by the more rapid heating of the 1 mil gage. The 3 mil curve lies slightly below (~4%) the 5 mil curve. Although the 3 and 5 mil gage will have different electrical resistances (greater for the thinner material), they resemble each other and differ from the 1 mil gage in having a smaller temperature increase from immersion in the hot gases; the smaller amount of heating also means a lower heat effect on the electrical conductivity. The 5 mil gage was used in this study to minimize conduction effects and still give a reasonable rise time, i.e., less than 125 ns.

Evaluation of Single Record Results. As stated above, one objective of this work was to search for a break in the initial part of individual u,t records. Breaks\* at  $t \leq 200$  ns were observed in 18 of the 22 acceptable records (see

\*This terminology is used to denote a marked change of slope of the oscilloscope trace.

Table 2 and Figure 3 for an example). In ten of these records (for six shots), two closely spaced breaks were observed at  $0 < t \leq 200$  ns (see points A and B in Figure 4). This structure in the records was not entirely unexpected for two reasons: (1) Craig<sup>5</sup> observed two breaks in his curves relating free surface velocity and distance and (2) earlier computational work on rise time<sup>1,2</sup> implied that the recording systems might cause one break to appear as two. Experimental determination of the cause of the twin breaks would require a rise time of  $\leq 20$  ns or, equivalently, a 1 mil EMV gage. It was shown above (Figure 2) that a gage of this thickness was ineffective in high density pressed TNT; hence an experimental investigation with better time resolution is not feasible. After an examination of the  $u, t$  values obtained at points A, B and C (values of A and B are listed in the appendix), we concluded that those from point C were the most reasonable C-J values. Moreover, we believe that the form of the output, i.e., the existence of point C, probably results from distortion of the input by the recording system. This is certainly expected when the total rise time is greater than half the time to point C (see analysis of reference 1) as turns out to be the case in the present measurements.

Table 2 lists the values of  $u$  and  $\gamma$  obtained at the break in individual records. As mentioned above, when two breaks appear, point C is associated with the C-J point. There are two values for some shots because a record was obtained from both oscilloscopes.

Another method for obtaining the C-J point using single records is to compare the experimental  $u, t$  curves with detonation product expansion curves calculated from the plane Taylor wave theory.<sup>6</sup> The calculated  $u, t$  curve is a good approximation to the experimental curve in the region from the  $u_{CJ}$  break to the break at 600 ns (see section below, Appearance of Additional Break at  $\approx 600$  ns). The results obtained by this method are listed in Table 3. These results agree with those of Table 2 to within  $\pm 1\%$ , and thereby support our interpretation of the records and their reduction. The  $u, t$  curves for  $x = 25.4$  mm are omitted from Table 3 because the particle velocity was still building up to its steady state at this station (see section below, Buildup of Particle Velocity with Charge Length).

In order to check these values further, shots were fired with the EMV gage located at the interface between pressed TNT and PMMA. As can be seen from Figure 5, a sharp break also occurs in this record. Since the EMV gage records the particle velocity of the PMMA, an impedance matching calculation has to be performed to obtain the particle velocity in the TNT gases which corresponds to the break point. Figure 6 shows this calculation for  $x = 25.4$  mm. The line labeled TNT has the slope  $10 \cdot \rho_0 \cdot D$  where  $\rho_0 = 1.60$  gm/cc and  $D = 6.91$  mm/ $\mu$ sec. The line labeled PMMA is the PMMA Hugoniot.<sup>7</sup> The dashed line labeled 1 has a slope equal to  $-10 \cdot \rho_0 \cdot D$  and passes through the PMMA line at  $u = 2.08$  mm/ $\mu$ sec (value at break of Figure 5). This yields a first approximation to  $u_{CJ}$  of 1.67 mm/ $\mu$ sec (point A). Using this value to calculate  $\gamma$ , we drew the isentrope (dashed curve 2) which corresponds to this approximate  $u_{CJ}$  and which passes through 2.08 mm/ $\mu$ sec on the PMMA curve. This yields a new value of  $u_{CJ}$  equal to 1.63 mm/ $\mu$ sec which is in good agreement with the results in Table 2. For  $x = 76.2$  mm (shot #217), a value of 1.72 mm/ $\mu$ sec was obtained for  $u_{CJ}$  which is 2.5% greater than the values listed in Table 2. Part of this discrepancy may be due to noise which makes determination of the exact break

point difficult from the record of the  $x = 76.2$  mm interface shot. All of the above discussion leads to the conclusion that single record results are quite consistent.

Pair Comparison of  $u, t$  Curves. In the study of cast TNT<sup>6</sup>, the method used to determine the C-J point was to compare the  $u, t$  curves for several values of  $x$  and determine the point beyond which the curves diverge. We have used essentially the same approach here except the  $u, t$  curves were compared two at a time; and, as in the previous section,  $x \geq 38.1$  mm. The  $u, t$  curves were shifted along the time axis until the initial portion coincided; this procedure is justified since the presence of any noise and changes in intensity of the oscilloscope trace made the  $t = 0$  point uncertain by  $\pm 20$  ns. The point of divergence of the two curves is then taken as the C-J point for that pair of curves. The results of this process are listed in Table 4. Shot 206 ( $x = 38.1$  mm) was not included because it appears to exhibit a slight overshoot\*; this is based on the fact that its  $u, t$  curve lies above that for  $x = 50.8$  and  $76.2$  mm. Shot 214 was also omitted because of a large irregularity in the early part of the record. This pair comparison approach was also applied to cast TNT records (see Appendix).

Consideration of Different Record Treatments. The four methods that have been used to obtain  $u_{CJ}$  and  $\tau_{CJ}$  yield consistent results which are listed in Table 5. The overall average values obtained at the C-J point are  $u_{CJ} = 1.72$  mm/ $\mu$ sec and  $\tau_{CJ} = 141$  ns. Hence the interpretation of the single break (or point C) on the shot record as corresponding to the C-J point is reinforced by the concept of propagation of a steady-state structure unchanging with  $x \geq 38$  mm, followed by an expansion (non-steady state) which is well reproduced by the Taylor wave computation. The agreement of the three treatments used on the records of measurements made in TNT also affirms the applicability of the usual detonation theory in this experiment as does obtaining the same result in interface measurements of TNT/PMMA systems.

The data in Table 2 show that the maximum difference in two records (two oscilloscopes) of the same shot are  $0.03$  mm/ $\mu$ sec and  $30$  ns in  $u$  and  $\tau$  respectively. These are within the errors to be expected in record reading,  $\pm 1\%$  in  $u$  and  $\pm 20$  ns in  $\tau$ . On the other hand, the maximum differences between replicate shots are  $0.07$  mm/ $\mu$ sec (only  $0.02$  mm/ $\mu$ sec can be accounted for by the density variation of  $\pm 0.01$  gm/cc) and  $75$  ns, about 2.5 times as large. Thus the error that can be caused by charge variation seems somewhat greater than that to be expected from record reading.

If the data for four shots at  $x = 25.4$  mm and four at  $x = 76.2$  mm are combined with the appropriate interface measurements, the 2 five-shot data sets have about the same  $\sigma$  value. As would be expected each result is included in the range average  $u_{CJ} \pm 2\sigma$ . The value of  $2\sigma$  is  $0.05 - 0.06$  mm/ $\mu$ sec and is probably applicable to the whole range of  $x$ . A similar treatment of sets of  $\tau$  in Table 2 gives  $\sigma$  values of  $24$  and  $14.4$  ns at  $x = 25.4$  and  $76.2$  mm, respectively. The latter value should be more applicable to the steady state and its limits would

---

\*The  $u_{CJ}$  value for this shot was only about 2% higher than the average of the single-shot determinations. However, the pair matching procedure has the disadvantage of overemphasizing the effect of a single high (or low) result. It has the advantage of decreasing the range in the values of  $\tau$  obtained. Compare the results of Tables 2 and 4.

be approximately  $\tau_{CJ}$  (average)  $\pm 30$  ns. Both limits cover the range shown in Table 5; they amount to about  $\pm 3.5\%$  in  $u$  and  $\pm 21\%$  in  $r$ .

**Buildup of Particle Velocity with Charge Length.** Figure 7 shows particle velocity at the breaks in the oscilloscope records, as discussed above, as a function of  $x$ . The boxes show the  $2\sigma$  ranges; the solid line, our average value of  $u_{CJ}$  as determined in the preceding section. Although the  $\sigma$  value does not demonstrate a significant difference between the results at  $x = 25.4$  and  $76.2$  mm, it does show that the former is significantly less than the average value of  $1.72$  mm/ $\mu$ sec. Moreover, it is reasonable to expect a buildup to steady state, such as that indicated by the dashed line of Figure 7, since the computed particle velocity at  $x = 0$  is  $1.35$  as compared to  $1.72$  mm/ $\mu$ sec at steady state. Run-lengths of up to two charge diameters have been observed in the dimensions of the NOL large scale gap test when the acceptor is unconfined, as it is here.<sup>8</sup> Of course, the run-length depends on the strength of the initiating shock and the shock sensitivity of the material. A run-length of over half a diameter was not expected for an entering shock as high as  $110$  kbar in pressed TNT. It is evident that this point must be checked in any future experiments.

**Appearance of Additional Break at  $\approx 600$  ns.** Previous work in cast TNT<sup>6</sup> showed that breaks occurred at  $t \approx 600$  ns; that is, the slope of the  $u, t$  curve became markedly steeper at that time. The tentative explanation given then was that perhaps only 99% of the TNT had reacted after the measured reaction time of about 300 ns, the last 1% reacting during the next 300 ns. The  $u, t$  curves for pressed TNT for  $x \geq 38.1$  mm also show these breaks at  $t \approx 600$  ns. In fact, they also appear in records from Teteryl,  $\rho_0 = 1.51$  gm/cc, at approximately the same time.<sup>6</sup> Since the charge geometry and dimension were the same for all three different explosives, a more probable cause of these breaks than tailing-off reaction is the flow pattern behind the C-J plane. Specifically, these breaks may be occurring when the gases at the gage acquire velocity components in radial directions, i.e., when the flow is no longer one dimensional.

#### COMPARISON OF PRESSED AND CAST TNT

The EMV gage study has revealed a significant difference in the C-J parameters of 50.8 mm diameter cast and pressed TNT at approximately the same density. It is impossible to say whether the same difference would be found in much larger charges. The present results are listed in Table 6. Although the detonation velocity of pressed TNT is only 1% higher than that of cast TNT,  $u_{CJ}$  is 7.5% higher and the C-J pressure,  $P_{CJ}$ , is 6.8% higher than that of cast TNT.  $P_{CJ}$  was calculated using

$$P_{CJ} = 10 \cdot \rho_0 \cdot u_{CJ} \cdot D$$

where the units of  $\rho_0$ ,  $u_{CJ}$ , and  $D$  are, respectively, gm·cm<sup>-3</sup>, mm· $\mu$ sec<sup>-1</sup>, and mm· $\mu$ sec<sup>-1</sup>. The reaction time,  $\tau_{CJ}$ , of the pressed TNT is half that of cast TNT. Also the break associated with the C-J point is sharper in pressed TNT; so much sharper, in fact, that it can be used to determine the C-J parameters from the record of a single shot.

The buildup of particle velocity observed in pressed TNT was not observed in cast TNT where a different booster system was used. Jacobs<sup>10</sup> had already shown that it requires a greater thickness of cast TNT as compared to pressed TNT to reach steady state detonation velocity. With this in mind, an intermediate layer of more sensitive explosive was placed between the PWB and cast TNT.<sup>6</sup>

#### COMPARISON WITH PREVIOUS PRESSED TNT RESULTS

The C-J parameters of pressed TNT ( $\rho_0 = 1.60$  gm/cc) have been in dispute for several years (see above). Table 7 lists our results along with those obtained by Dremin<sup>4</sup> and Craig<sup>5</sup>. Our value for  $u_{CJ}$  is 6% higher than Dremin's. Dremin claims an accuracy of 5% while our experimental precision is  $\leq 3.5\%$ ; for a five shot set of measurements,  $\sigma \sim 2\%$ . A possible reason for the discrepancy is that we were able to observe the C-J break in our records while Dremin could not. Thus Dremin had to extrapolate to some value of  $r$  (probably 100 ns) in order to obtain a value of  $u$  which he identified as  $u_{CJ}$ . Considering this fact and the quality of his oscilloscopes (rise time of  $\sim 60$  ns), our results are in fair agreement with Dremin's although we expect our results to be the more accurate.

The  $u_{CJ}$  value, derived from Craig's reported value of  $P_{CJ}$  measured in 50.8 mm diameter charge of TNT ( $\rho_0 = 1.63$  gm/cc), is 7% higher than ours. When Craig's value is adjusted\* to a density of 1.60 gm/cc, it becomes 1.33 mm/ $\mu$ sec or 6.4% higher than our value.

The present work therefore produces a value about 6% higher than Dremin's and about 6% lower than Craig's. Inasmuch as 6% is also the order of magnitude of the experimental error, the present result cannot resolve the current discrepancy in the value of  $u_{CJ}$  for pressed TNT.

As we mentioned earlier, Craig observed two breaks in his plots of peak free surface velocity vs thickness of driven metal plates. He used the first break to determine  $P_{CJ}$ . The second break was attributed to the end of a "decay zone", the start of which was associated with the first break. If it is assumed that Craig should have used his second break, the resulting value of  $P_{CJ}$  is 184.5 kbar which corresponds to  $u_{CJ}$  of 1.63 mm/ $\mu$ sec. When these values are adjusted to  $\rho_0$  of 1.59 gm/cc, they become 177 kbar and 1.62 mm/ $\mu$ sec, respectively. The adjusted values are in excellent agreement with Dremin's at a charge diameter of 60 mm. Petrone<sup>11</sup> has already pointed out the excellent agreement found for infinite diameter charges, and has argued, as does Dremin, that the correct break to associate with C-J conditions is the second. Again the present results cannot resolve the problem.

\*For adjustment, we used

$$\frac{P_1}{P_2} = \frac{\rho_1 D_1^2}{\rho_2 D_2^2}$$

and

$$u_1 = P_1 / (\rho_1 D_1)$$

and adjusted  $D$  for  $\rho$  with Equation (3) from Physics Fluids 4 (2), 262-274 (1961).

For completeness, it should be mentioned that Davis and Venable<sup>12</sup> have discussed the C-J pressure of Comp B-3 obtained using four different methods (see Table 8) and found that free surface measurements gave results which were 10-18% higher than embedded foil and rarefaction velocity measurements. Davis and Venable point out that "...perhaps the difficulty is really that we do not know how to make true pressure measurements."<sup>12</sup> Dremine<sup>4</sup> has pointed out that free surface velocity measurements should include a spill plane. Using this technique, Dremine obtained a  $u_{CJ}$  for pressed TNT of 1.61 mm/ $\mu$ sec.

### SUMMARY AND CONCLUSIONS

The C-J parameters of pressed TNT ( $\rho_0 = 1.60$  gm/cc, 50.8 mm diameter) determined in this study are:

$$u_{CJ} = 1.72 \text{ mm}/\mu\text{sec}$$

and

$$\tau_{CJ} = 141 \text{ ns.}$$

These values are greater than those given in the Russian literature<sup>3,4</sup>; the difference may be due to inferior instrumentation of the Russians. These results are lower than Craig's<sup>5</sup> as he interpreted his data (and are, of course, higher than the values based on the second break he observed, i.e., those in agreement with the Russian results).

An important conclusion of this work is that a break in a single record can be used to obtain  $u_{CJ}$  to within  $\pm 4\%$  and  $\tau_{CJ}$  to within  $\pm 30$  ns. Similar conclusions have been drawn using tetryl<sup>9</sup> ( $\rho_0 = 1.51$  gm/cc) for which  $\tau_{CJ} \approx 100$  ns. The conditions for using single record results to determine the C-J parameters is that the rise time of the system be  $\leq \frac{1}{2}$  the time to the break. For explosives with a long reaction time one would want a long run length to assure a flat Taylor wave. The value of  $u_{CJ}$  can be readily checked using Taylor wave theory for one-dimensional flow with a constant gamma. This study, along with that for cast TNT, has shown that this calculation is a good approximation to the flow in the region from the C-J break to the break at  $\approx 600$  ns. It also confirms the classical structure of the steady state detonation wave.

# REFERENCES

1. S. J. Jacobs and D. J. Edwards, "Experimental Study of the Electromagnetic Velocity Gage Technique," Preprints, 5th Symposium (International) on Detonation, Pasadena, Cal., (323-334) ONR Rept. DR-163 (August 1970).
2. D. J. Edwards, J. O. Erkman, and S. J. Jacobs, "The Electromagnetic Velocity Gage and Applications to the Measurement of Particle Velocity in PMMA," NOLTR 70-79 (20 July 1970).
3. A. N. Dremin and K. K. Shvedov, "The Determination of Chapman-Jouguet Pressure and of the Duration of Reaction in the Detonation Wave of High Explosives," Zh. Prikl. Mekhan. i Tekhn. Fiz., 1964 (2), 154-159.
4. V. A. Veretennikov, A. N. Dremin, O. K. Rozanov, and K. K. Shvedov, "Applicability of Hydrodynamics Theory to the Detonation of Condensed Explosives," Combustion, Explosion, and Shock Waves, 3(1), 1-6 (1967).
5. B. G. Craig, "Measurements of the Detonation Front Structure in Condensed-Phase Explosives," 10th Symp. (Int.) on Combustion, pp 863-867, the Combustion Institute, Pittsburgh, Penna., (1965).
6. D. J. Edwards and J. O. Erkman, "The Measurement of Particle Velocity in Cast TNT," NOLTR 71-19 (14 June 1971).
7. B. Hayes and J. N. Fritz, "Measurement of Mass Motion in Detonation Products by an Axially-Symmetric Electromagnetic Technique," Preprints, 5th Symposium (International) on Detonation, Pasadena, Cal., ONR Rept. DR-163 (August 1970).
8. D. Price, J. P. Toscano and I. Jaffe, "Development of the Continuous Wire Method Progress Report III. Measurements in Cast DINA." NOLTR 67-10 (20 April 1967).
9. D. J. Edwards, J. O. Erkman and D. Price, NOLTR 72-83.
10. S. J. Jacobs, T. P. Liddiard, Jr. and B. E. Drimmer, "The Shock-to-Detonation Transition in Solid Explosives," 9th Symp. (Int.) on Combustion, pp 517-529, Academic Press, Inc., New York, New York, (1963)
11. F. J. Petrone, "Validity of the Classical Detonation Wave Structure for Condensed Explosives," The Physics of Fluids, 11(7), 1473-1476 (July 1968).
12. W. C. Davis and D. Venable, "Pressure Measurements for Composition B-3," Preprints, 5th Symposium (International) on Detonation, Pasadena, Cal., ONR Rept. DR-163 (August 1970).



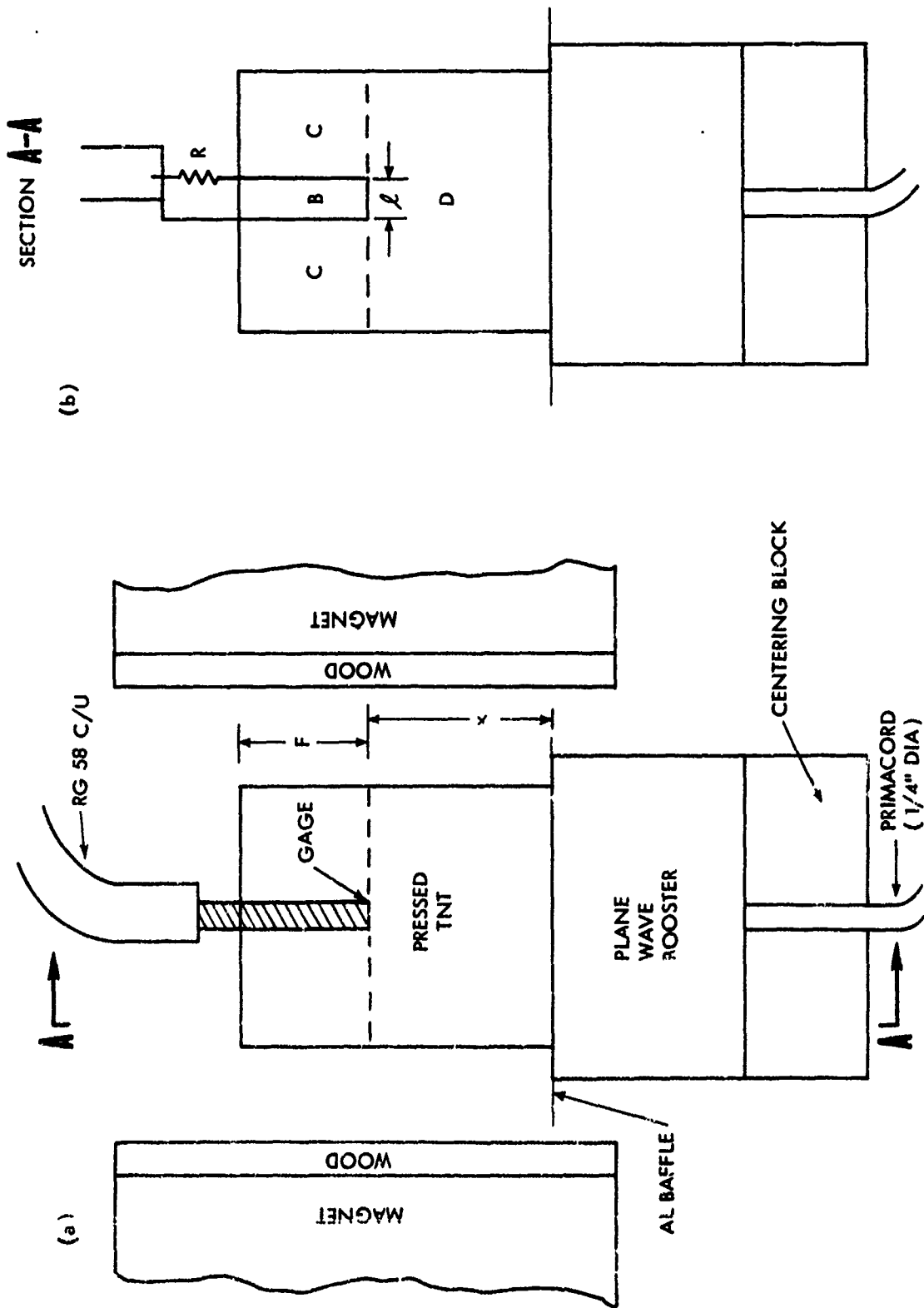


FIG. 1 EXPERIMENTAL SETUP

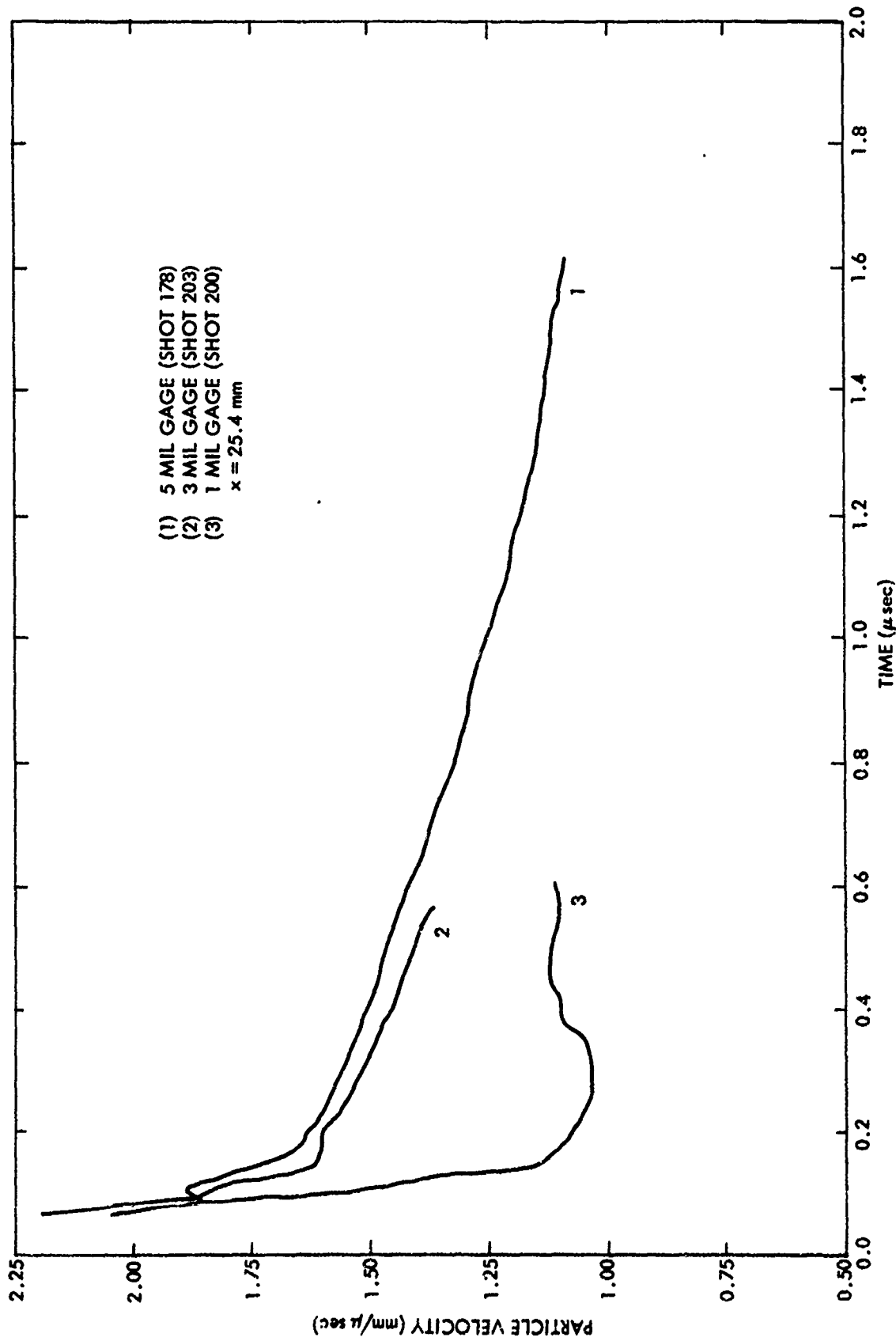


FIG. 2 COMPARISON OF DIFFERENT THICKNESS EMV GAGES

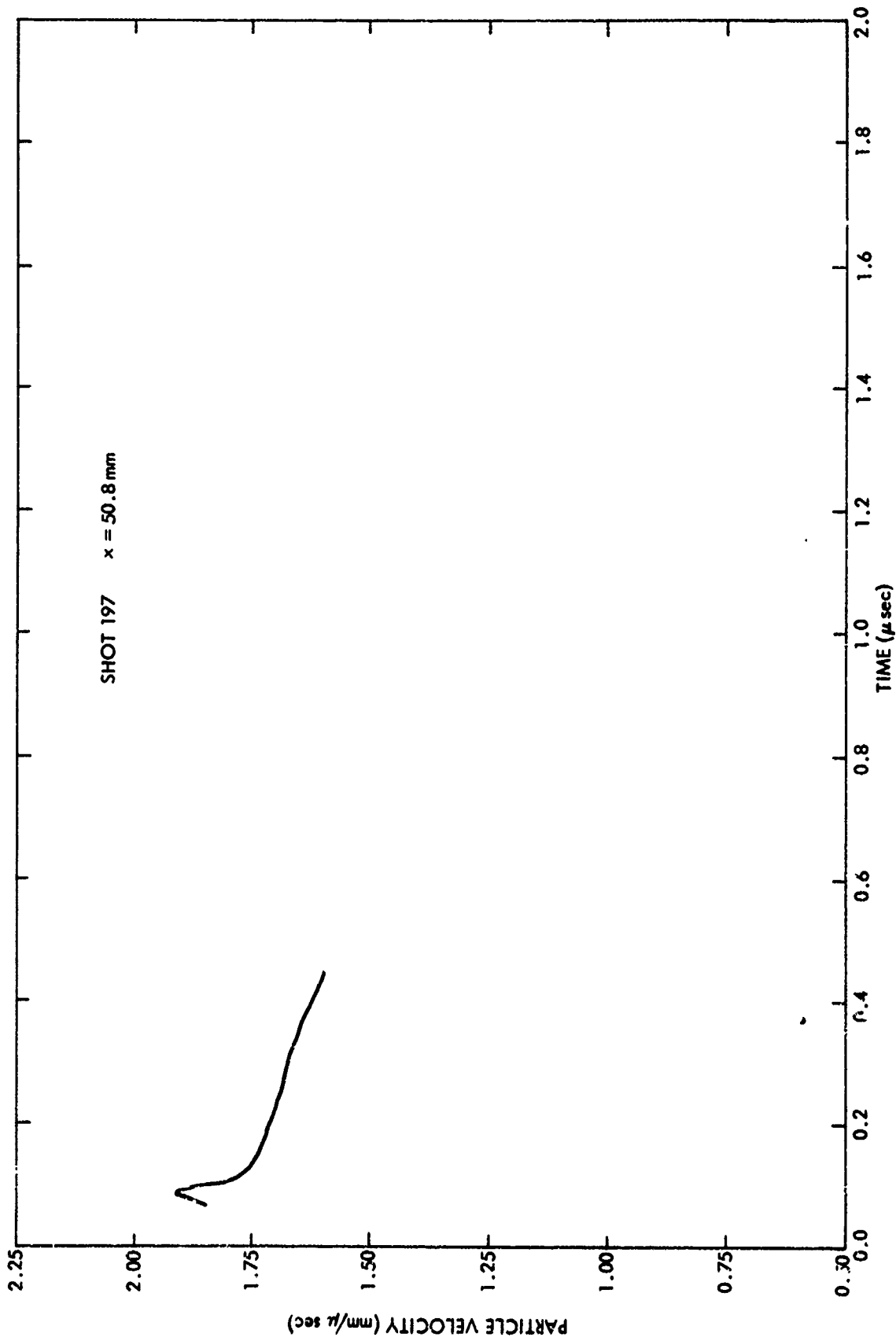


FIG. 3  $u, t$  CURVE WITH ONE BREAK

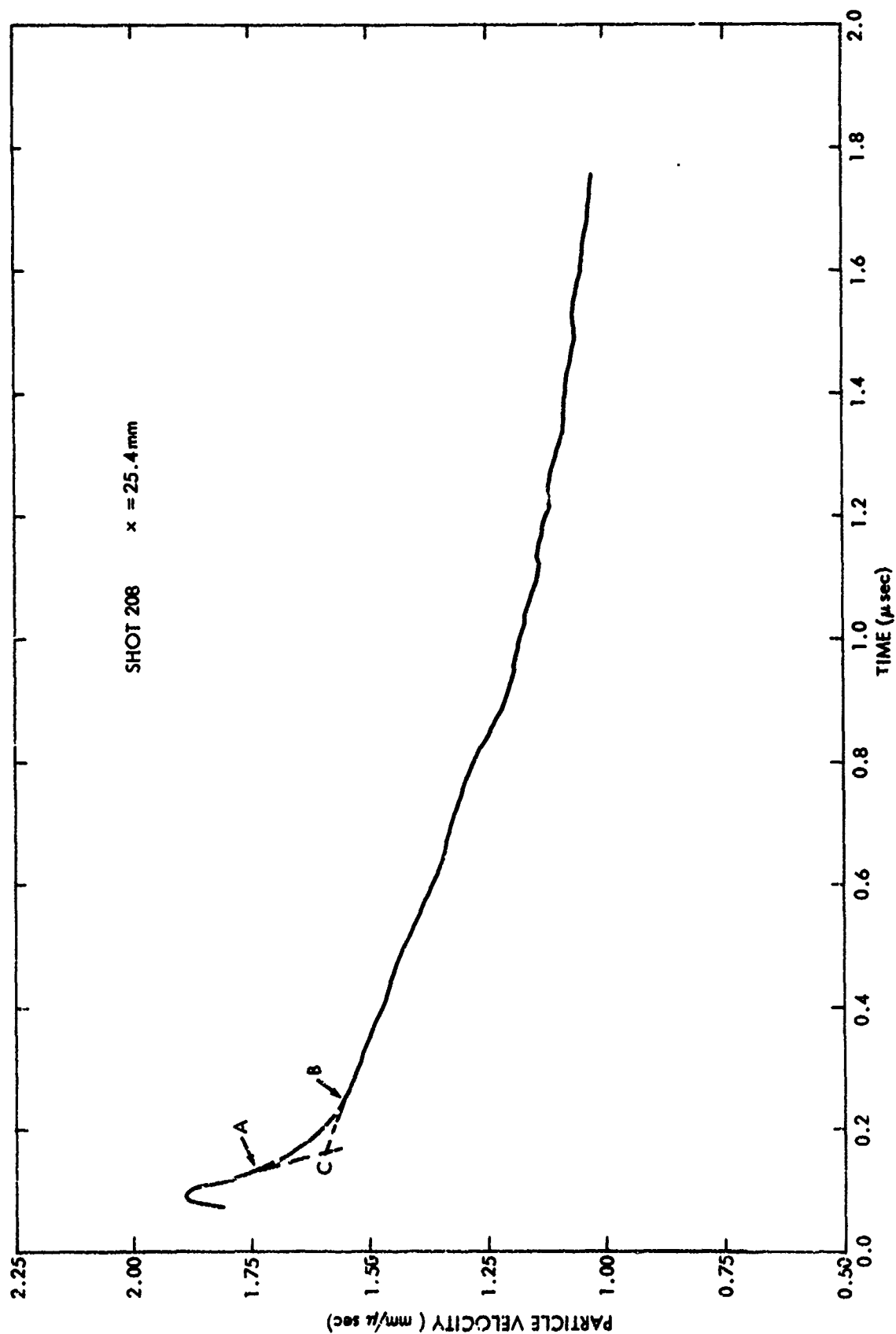


FIG. 4 u, t CURVE WITH TWO BREAKS

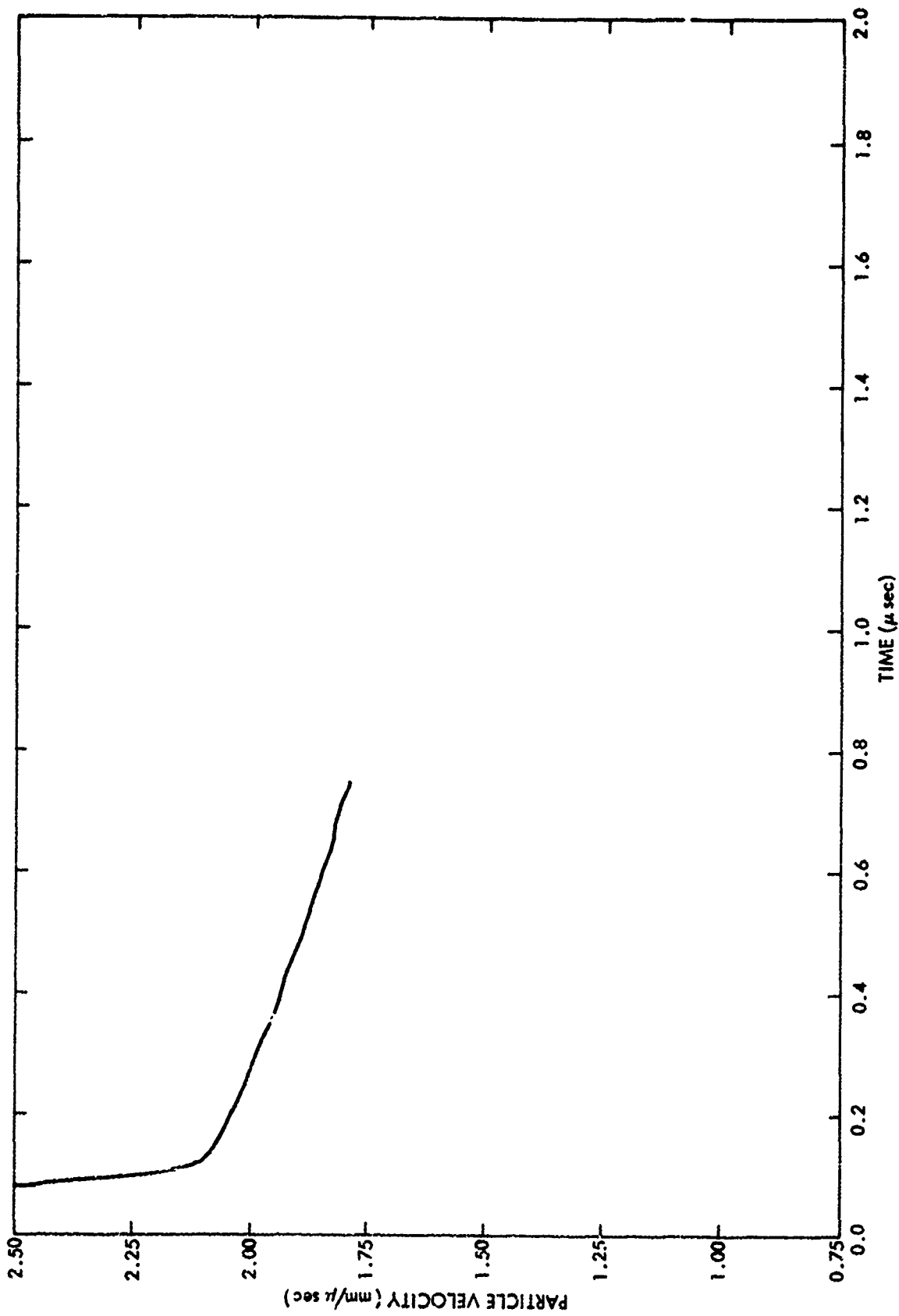


FIG. 5 TNT/PMMA INTERFACE RESULT (  $x \approx 25.4 \text{ mm}$  )

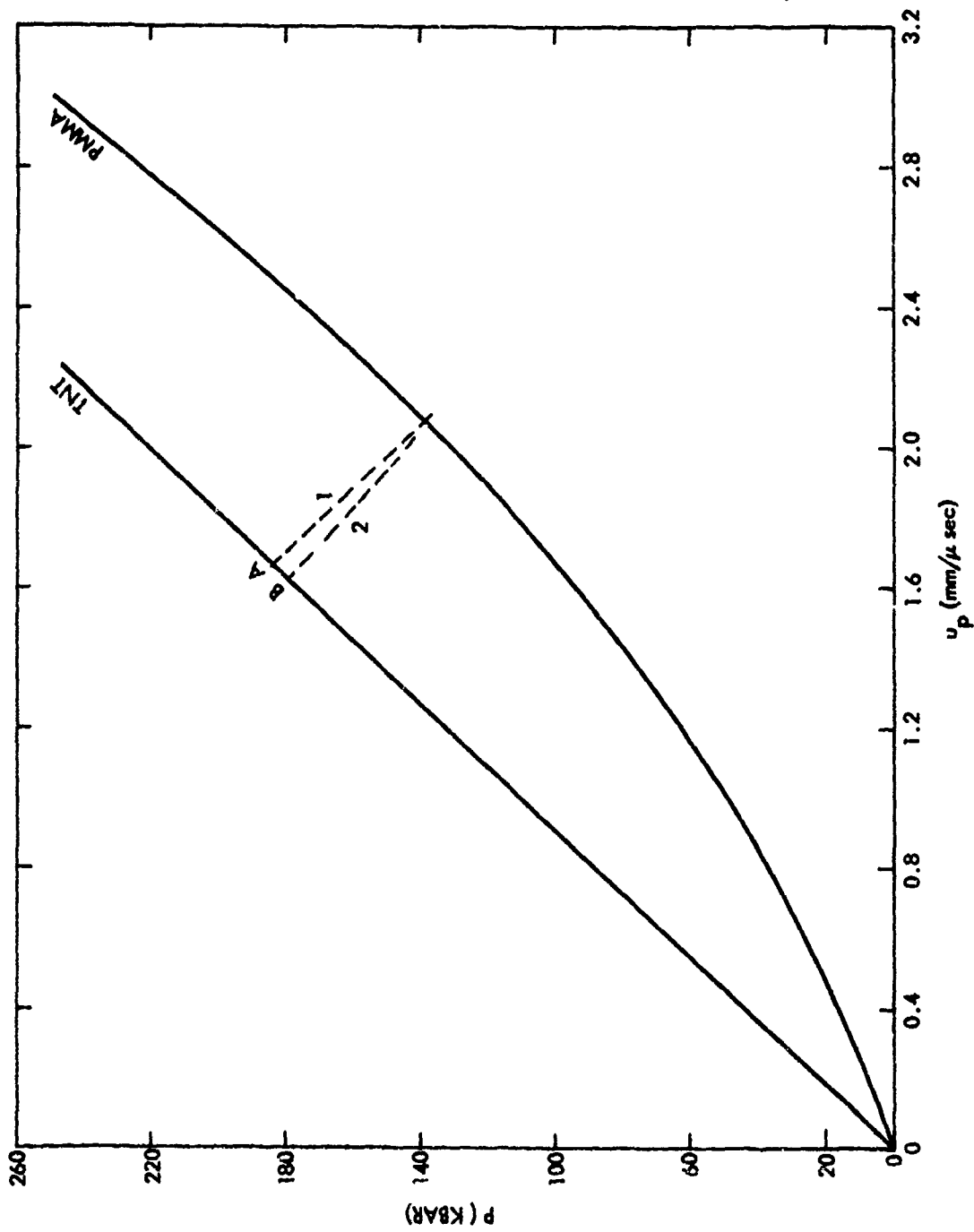


FIG. 6 IMPEDANCE MATCHING CALCULATION FOR PRESSED TNT/PMMA INTERFACE RESULT ( $x \approx 25.4$  mm)

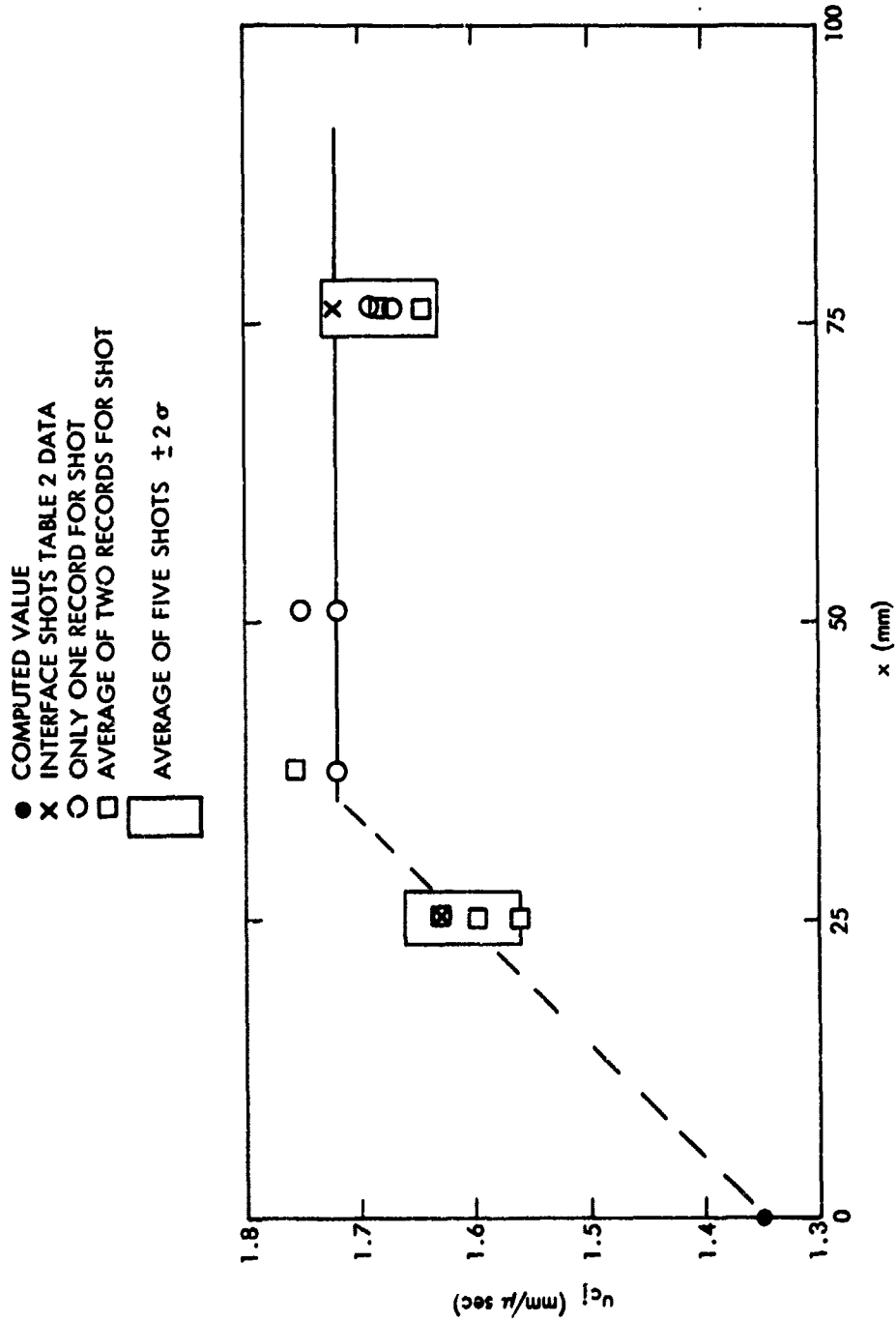


FIG. 7 C-J PARTICLE VELOCITY VS DISTANCE

Table 1

## List of Individual Experiments

| <u>x<sub>1</sub></u><br><u>mm</u> | <u>Shot</u><br><u>No.</u> | <u>Dia.</u><br><u>mm</u> | <u>PWB</u><br><u>Dia.</u><br><u>mm</u> |
|-----------------------------------|---------------------------|--------------------------|--|
| <u>5 mil Gage</u>                 |                           |                          |  |
| 25.4                              | 172                       | 50.8                     | 63.5                                   |
| 25.4                              | 176                       | 50.8                     | 50.8                                   |
| 25.4                              | 177                       | 50.8                     | 50.8                                   |
| 25.4                              | 178                       | 50.8                     | 50.8                                   |
| 25.4                              | 198                       | 50.8                     | 63.5                                   |
| 25.4                              | 199                       | 50.8                     | 63.5                                   |
| 25.4                              | 208*                      | 63.5                     | 63.5                                   |
| 38.1                              | 206*                      | 50.8                     | 50.8                                   |
| 38.1                              | 213*                      | 50.8                     | 50.8                                   |
| 50.3                              | 190                       | 50.8                     | 50.8                                   |
| 50.8                              | 191                       | 50.8                     | 50.8                                   |
| 50.8                              | 197                       | 50.8                     | 50.8                                   |
| 76.2                              | 207*                      | 50.8                     | 50.8                                   |
| 76.2                              | 214*                      | 50.8                     | 50.8                                   |
| 76.2                              | 215*                      | 50.8                     | 50.8                                   |
| 76.2                              | 216*                      | 50.8                     | 50.8                                   |
| <u>3 mil Gage</u>                 |                           |                          |  |
| 25.4                              | 201                       | 50.8                     | 63.5                                   |
| 25.4                              | 203                       | 50.8                     | 63.5                                   |
| <u>1 mil Gage</u>                 |                           |                          |  |
| 25.4                              | 200                       | 50.8                     | 63.5                                   |
| <u>TNT/PMMA Interface</u>         |                           |                          |  |
| 25.4                              | 184                       | 50.8                     | 50.8                                   |
| 25.4                              | 193                       | 50.8                     | 50.8                                   |
| 76.2                              | 217                       | 50.8                     | 50.8                                   |

\*Constant Current Supply



NOLTR 72-82

Table 2

C-J Values Obtained from Break Point on Individual Records

| <u>x</u><br>mm | <u>Shot</u><br><u>No.</u> | <u>u</u><br>mm/<br><u>μsec</u> | <u>τ</u><br>ns | <u>Oscillo-</u><br><u>scope</u> |
|----------------|---------------------------|--------------------------------|----------------|---------------------------------|
| 25.4           | 172                       | 1.63                           | 120            | HP 175                          |
| 25.4           | 177                       | 1.56                           | 170            | Tek 454                         |
| 25.4           | 177                       | 1.56                           | 195            | HP 175                          |
| 25.4           | 178                       | 1.63*                          | 170*           | HP 175                          |
| 25.4           | 178                       | 1.63*                          | 180*           | Tek 454                         |
| 25.4           | 208                       | 1.60*                          | 155*           | HP 175                          |
| 25.4           | 208                       | 1.60*                          | 165*           | Tek 454                         |
| 38.1           | 206                       | 1.74*                          | 145*           | Tek 454                         |
| 38.1           | 206                       | 1.77*                          | 140*           | HP 175                          |
| 38.1           | 213                       | 1.72*                          | 100*           | Tek 454                         |
| 50.8           | 190                       | 1.72*                          | 150*           | HP 175                          |
| 50.8           | 197                       | 1.75                           | 120            | Tek 454                         |
| 76.2           | 207                       | 1.64*                          | 140*           | HP 175                          |
| 76.2           | 207                       | 1.65*                          | 170*           | Tek 454                         |
| 76.2           | 214                       | 1.67                           | 190            | Tek 454                         |
| 76.2           | 215                       | 1.68                           | 175            | HP 175                          |
| 76.2           | 215                       | 1.68                           | 190            | Tek 454                         |
| 76.2           | 216                       | 1.69                           | 190            | Tek 454                         |

\*Point C

Table 3

$u_{CJ}$  Values Obtained by Method of Plane Taylor Wave Comparisons

| $x$<br><u>mm</u> | Shot<br><u>No.</u> | $u_{CJ}$<br><u>mm/<math>\mu</math>sec</u> |
|------------------|--------------------|---|
| 38.1             | 213                | 1.70                                      |
| 38.1             | 205                | 1.75                                      |
| 50.8             | 190                | 1.725                                     |
| 50.8             | 197                | 1.725                                     |
| 76.2             | 207                | 1.65                                      |
| 76.2             | 214                | 1.67                                      |
| 76.2             | 215                | 1.67                                      |

Table 4  
Pair Comparison of u,t Curves

| <u>x</u><br>mm            | <u>Shot</u><br><u>No.</u> | <u>x</u><br>mm | <u>Shot</u><br><u>No.</u> | <u>u<sub>CJ</sub></u><br>mm/<br>μsec | <u>r</u><br>ns |
|---------------------------|---------------------------|----------------|---------------------------|--------------------------------------|----------------|
| <u>Individual Results</u> |                           |                |                           |                                      |                |
| 38.1                      | 213                       | 50.8           | 197                       | 1.75                                 | 110, 120       |
| 38.1                      | 213                       | 50.8           | 190                       | 1.73                                 | 120, 160       |
| 38.1                      | 213                       | 76.2           | 207                       | -                                    | -              |
| 38.1                      | 213                       | 76.2           | 215                       | 1.70                                 | 130, 160       |
| 50.8                      | 197                       | 76.2           | 207                       | 1.75                                 | 120, 120       |
| 50.8                      | 197                       | 76.2           | 215                       | 1.75                                 | 120, 140       |
| 50.8                      | 190                       | 76.2           | 207                       | 1.73                                 | 130, 160       |
| 50.8                      | 190                       | 76.2           | 215                       | 1.73                                 | 160, 160       |

Average results for x = 38.1 to 76.2

$u_{CJ} = 1.73 \text{ mm}/\mu\text{sec}$

$r = 136 \text{ ns}$

Table 5  
Overall Results for Pressed TNT

| x<br>mm            | $\frac{dCJ}{dx}$<br>mm/msec |             |           |       | r<br>ns |      |
|--------------------|-----------------------------|-------------|-----------|-------|---------|------|
|                    | Break                       | Taylor Wave | Interface | Pair* | Break   | Pair |
| 35.1               | 1.74                        | 1.73        | -         |       | 121     |      |
| 50.8               | 1.74                        | 1.73        | -         |       | 135     |      |
| 76.2               | 1.67                        | 1.66        | 1.72      |       | 179     |      |
| Overall<br>Average | 1.72                        | 1.70        | 1.72      | 1.73  | 145     | 136  |

\*Does not include shots 206 and 214

Table 6  
Detonation Parameters of Cast and Pressed TNT

|  | <u>Pressed</u>  | <u>Cast</u> <sup>6</sup> |
|--|-----------------|--------------------------|
| Density<br>gm/cc                       | $1.60 \pm 0.01$ | $1.62 \pm 0.01$          |
| Detonation Velocity<br>mm/ $\mu$ sec   | (6.91)          | 6.85                     |
| C-J Particle Velocity<br>mm/ $\mu$ sec | 1.72            | 1.60                     |
| C-J Pressure<br>Kbar                   | 190             | 178                      |
| Reaction Time ( $\tau_{CJ}$ )<br>ns    | 141             | 300                      |

Table 7

Comparison of Pressed TNT Results

|                                       | <u>Present<br/>Results</u> | <u>Dremin<sup>4</sup></u> | <u>Craig<sup>5*</sup></u> |              |
|---------------------------------------|----------------------------|---------------------------|---------------------------|--------------|
|                                       |                            |                           | 1st<br>Break              | 2nd<br>Break |
| Density<br>gm/cc                      | 1.60                       | 1.59                      | 1.63                      | 1.63         |
| Detonation<br>Velocity, mm/ $\mu$ sec | (6.91)                     | 6.91                      | (6.94)**                  | (6.94)**     |
| $u_{CJ}$<br>mm/ $\mu$ sec             | $1.72 \pm 0.05$            | $1.62 \pm 0.08$           | (1.84)                    | (1.63)       |
| $P_{CJ}$<br>Kbar                      | 190                        | 178                       | 208.5                     | 184.5        |
| $r_{CJ}$<br>ns                        | $141 \pm 30$               | <100                      | -                         | -            |

\*50.8 mm dia. results

\*\*D Computed from Equation (3), Phys. Fluids 4(2), 262-274 (1961)

Table 8

Measured Pressure For Composition B-3\*

| <u>Technique</u>               | <u>Pressure (Kb)</u> |
|--------------------------------|----------------------|
| Rarefaction Velocity (PHERMEX) | 368 ± 6              |
| Embedded Foils (PHERMEX)       | 275 ± 4              |
| Protected Flash Gap            | 292 ± 5              |
| Reflection-change Flash Gap    | 312 ± 5              |

---

\*Table 1, Reference (12)

## APPENDIX

Supplementary Data. Table A1 lists the shots for which two breaks appeared on the records (Points A and B, see Figure 4) and the values of  $u$  and  $\tau$  at these points.

Pair Comparison of Cast TNT. In the earlier study on cast TNT<sup>6</sup>, the method used to determine the C-J parameters was to compare the  $u, t$  curves for several values of  $x$ , determine the point beyond which the curves diverge, and associate it with the C-J point. The comparison of  $u, t$  curves by pairs incorporates the same idea but the time axis is adjusted until the initial part of the  $u, t$  curves coincides. This comparison has been carried out for the cast TNT experiments reported previously.<sup>6</sup> A total of 55 pair comparisons were made. These results are listed in Table A2. The overall average yields a  $u_{CJ} = 1.60$  mm/ $\mu$ sec which is exactly the value obtained before and a  $\tau_{CJ} = 270$  ns as compared to 300 ns obtained before. The fact that the difference in  $\tau_{CJ}$  is 30 ns is not surprising because of the difficulty in detecting a break in the  $u, t$  curves for cast TNT.



Table A1

Records with Two Breaks

| <u>x</u><br><u>mm</u> | <u>Shot</u><br><u>No.</u> | <u>Oscillo-</u><br><u>scope</u> | <u>Point A</u>             |                       | <u>Point B</u>             |                       |
|-----------------------|---------------------------|---------------------------------|----------------------------|-----------------------|----------------------------|-----------------------|
|                       |                           |                                 | <u>u</u><br><u>mm/μsec</u> | <u>r</u><br><u>ns</u> | <u>u</u><br><u>mm/μsec</u> | <u>r</u><br><u>ns</u> |
| 25.4                  | 178                       | HP175                           | 1.66                       | 165                   | 1.60                       | 225                   |
| 25.4                  | 178                       | Tek454                          | 1.71                       | 150                   | 1.61                       | 230                   |
| 25.4                  | 208                       | HP175                           | 1.71                       | 140                   | 1.57                       | 220                   |
| 25.4                  | 208                       | Tek454                          | 1.73                       | 140                   | 1.56                       | 230                   |
| 38.1                  | 206                       | Tek454                          | 1.87                       | 115                   | 1.72                       | 240                   |
| 38.1                  | 206                       | HP175                           | 1.89                       | 110                   | 1.75                       | 220                   |
| 38.1                  | 213                       | Tek454                          | 1.79                       | 90                    | 1.70                       | 130                   |
| 50.8                  | 190                       | HP175                           | 1.75                       | 140                   | 1.71                       | 190                   |
| 76.2                  | 207                       | HP175                           | 1.72                       | 130                   | 1.63                       | 200                   |
| 76.2                  | 207                       | Tek454                          | 1.74                       | 115                   | 1.64                       | 170                   |

Table A2

## Pair Comparison of Cast TNT

| <u>Shot<br/>No.</u> | <u>x+L<br/>mm</u> | <u>Shot<br/>No.</u> | <u>x+L<br/>mm</u> | <u>u<br/>mm/<math>\mu</math>sec</u> | <u>r<br/>ns</u> |
|---------------------|-------------------|---------------------|-------------------|-------------------------------------|-----------------|
| 155                 | 12.7              | 164                 | 19.1              | 1.53                                | 400, 300        |
|                     |                   | 163                 | 25.4              | 1.50                                | 340, 380        |
|                     |                   | 153                 | 25.4              | 1.50                                | 340, 400        |
|                     |                   | 161                 | 38.1              | 1.60                                | 270, 300        |
|                     |                   | 166                 | 38.1              | 1.66                                | 240, 280        |
|                     |                   | 144                 | 38.1              | 1.58                                | 260, 275        |
|                     |                   | 138                 | 38.1              | 1.59                                | 300, 275        |
|                     |                   | 130                 | 62.5              | 1.60                                | 290, 250        |
|                     |                   | 147                 | 62.5              | 1.59                                | 290, 300        |
|                     |                   | 131                 | 62.5              | -                                   | -               |
|                     |                   | 125                 | 76.2              | 1.59                                | 280, 280        |
|                     |                   | 148                 | 76.2              | -                                   | -               |
|                     |                   | 175                 | 76.2              | 1.59                                | 280, 280        |
|                     |                   | 163                 | 25.4              | 1.48                                | 340, 450        |
|                     |                   | 153                 | 25.4              | 1.48                                | 340, 450        |
|                     |                   | 161                 | 38.1              | 1.64                                | 180, 250        |
|                     |                   | 166                 | 38.1              | 1.60                                | 150, 240        |
|                     |                   | 144                 | 38.1              | -                                   | -               |
|                     |                   | 138                 | 38.1              | -                                   | -               |
| 164                 | 19.1              | 130                 | 62.5              | -                                   | -               |
|                     |                   | 147                 | 62.5              | -                                   | -               |
|                     |                   | 131                 | 62.5              | -                                   | -               |
|                     |                   | 125                 | 76.2              | 1.62                                | 120, 200        |
|                     |                   | 148                 | 76.2              | 1.70                                | 140, 140        |
|                     |                   | 175                 | 76.2              | 1.49                                | 280, 280        |
|                     |                   | 161                 | 38.1              | 1.60                                | 290, 300        |
|                     |                   | 166                 | 38.1              | 1.68                                | 250, 240        |
|                     |                   | 144                 | 38.1              | -                                   | -               |
|                     |                   | 138                 | 38.1              | 1.60                                | 300, 240        |
|                     |                   | 130                 | 62.5              | 1.64                                | 180, 200        |
|                     |                   | 147                 | 62.5              | 1.68                                | 250, 200        |
|                     |                   | 131                 | 62.5              | 1.45                                | 450, 400        |
|                     |                   | 125                 | 76.2              | 1.60                                | 300, 260        |
|                     |                   | 148                 | 76.2              | -                                   | -               |
|                     |                   | 175                 | 76.2              | 1.60                                | 300, 200        |
|                     |                   | 161                 | 38.1              | 1.60                                | 270, 260        |
|                     |                   | 166                 | 38.1              | 1.68                                | 240, 240        |
| 153                 | 25.4              | 144                 | 38.1              | 1.62                                | 275, 200        |
|                     |                   | 138                 | 38.1              | 1.62                                | 275, 200        |
|                     |                   | 130                 | 62.5              | 1.63                                | 270, 175        |
|                     |                   | 147                 | 62.5              | -                                   | -               |
|                     |                   | 131                 | 62.5              | -                                   | -               |
|                     |                   | 125                 | 76.2              | 1.62                                | 280, 240        |
|                     |                   | 148                 | 76.2              | -                                   | -               |
|                     |                   | 175                 | 76.2              | 1.60                                | 290, 190        |
| 163                 | 25.4              | 161                 | 38.1              | 1.60                                | 270, 260        |
|                     |                   | 166                 | 38.1              | 1.68                                | 240, 240        |
|                     |                   | 144                 | 38.1              | 1.62                                | 275, 200        |
|                     |                   | 138                 | 38.1              | 1.62                                | 275, 200        |
|                     |                   | 130                 | 62.5              | 1.63                                | 270, 175        |
|                     |                   | 147                 | 62.5              | -                                   | -               |
|                     |                   | 131                 | 62.5              | -                                   | -               |
|                     |                   | 125                 | 76.2              | 1.62                                | 280, 240        |
|                     |                   | 148                 | 76.2              | -                                   | -               |
|                     |                   | 175                 | 76.2              | 1.60                                | 290, 190        |

NOLTR 72-82

Table A2 (Cont.)

| <u>Shot<br/>No.</u> | <u>x+L<br/>mm</u> | <u>Shot<br/>No.</u> | <u>x+L<br/>mm</u> | <u>u<br/>mm/μsec</u> | <u>r<br/>ns</u> |
|---------------------|-------------------|---------------------|-------------------|----------------------|-----------------|
| 161                 | 38.1              | 130                 | 62.5              | -                    | -               |
|                     |                   | 147                 | 62.5              | 1.58                 | 300, 300        |
|                     |                   | 131                 | 62.5              | 1.61                 | 260, 250        |
|                     |                   | 125                 | 76.2              | 1.60                 | 320, 300        |
|                     |                   | 148                 | 76.2              | 1.60                 | 310, 260        |
|                     |                   | 175                 | 76.2              | 1.62                 | 270, 190        |
| 166                 | 38.1              | 130                 | 62.5              | 1.67                 | 260, 190        |
|                     |                   | 147                 | 62.5              | 1.64                 | 270, 250        |
|                     |                   | 131                 | 62.5              | -                    | -               |
|                     |                   | 125                 | 76.2              | 1.67                 | 260, 220        |
|                     |                   | 148                 | 76.2              | 1.67                 | 260, 200        |
|                     |                   | 175                 | 76.2              | 1.67                 | 260, 180        |
| 144                 | 38.1              | 130                 | 62.5              | 1.59                 | 275, 250        |
|                     |                   | 147                 | 62.5              | 1.57                 | 310, 325        |
|                     |                   | 125                 | 76.2              | -                    | -               |
|                     |                   | 148                 | 76.2              | 1.54                 | 270, 300        |
| 138                 | 38.1              | 130                 | 62.5              | -                    | -               |
|                     |                   | 147                 | 62.5              | 1.61                 | 340, 340        |
|                     |                   | 125                 | 76.2              | 1.56                 | 300, 300        |
|                     |                   | 148                 | 76.2              | 1.58                 | 300, 260        |
| 130                 | 62.5              | 125                 | 76.2              | 1.59                 | 260, 260        |
|                     |                   | 148                 | 76.2              | 1.59                 | 260, 250        |
| 147                 | 62.5              | 125                 | 76.2              | 1.56                 | 320, 300        |
|                     |                   | 148                 | 76.2              | -                    | -               |
|                     |                   | 175                 | 76.2              | 1.65                 | 220, 180        |
| 131                 | 62.5              | 125                 | 76.2              | 1.60                 | 260, 260        |
|                     |                   | 148                 | 76.2              | -                    | -               |
|                     |                   | 175                 | 76.2              | 1.65                 | 200, 180        |